BBC RD 1974/1

BBC

RESEARCH DEPARTMENT

REPORT

DIGITAL RECORDING USING HOLOGRAM ARRAYS: low-frequency micro-holograms on photographic film

K. Hacking, B.Sc.

Research Department, Engineering Division
THE BRITISH BROADCASTING CORPORATION January 1974

BBC RD 1974/1
UDC 621.397
621.377
535.8

DIGITAL RECORDING USING HOLOGRAM ARRAYS: LOW-FREQUENCY MICRO-HOLOGRAMS ON PHOTOGRAPHIC FILM

K. Hacking, B.Sc.

Summary

The report deals with the recording of small (micro) holograms, representing 'words' of binary-coded information, on conventional photographic film, and with the subsequent retrieval of this information. The work is the initial phase of a feasibility study of a possible system for recording digital television signals in real-time using laser-beam scanning combined with holographic techniques.

A theoretical analysis of holographic image formation is followed by the results of basic experiments and measurements on several film emulsions. The results show that binary storage densities of approximately 10^6 bits/cm^2 are feasible with average signal-to-interference ratios of 20 dB or better after reconstruction, and with hologram spatial bandwidths of less than 200 cycles/mm. At this storage density or greater, recording and replay could be achieved using laser radiation powers of less than 10 mW, assuming an optical efficiency greater than 10%.

issued under the authority of

P. Laing

Head of Research Department

Research Department, Engineering Division,
BRITISH BROADCASTING CORPORATION

January 1974

(PH-105)

DIGITAL RECORDING USING HOLOGRAM ARRAYS: LOW-FREQUENCY MICRO-HOLOGRAMS ON PHOTOGRAPHIC FILM

DIGITAL RECORDING USING HOLOGRAM ARRAYS: LOW-FREQUENCY MICRO-HOLOGRAMS ON PHOTOGRAPHIC FILM

K. Hacking, B.Sc.

List of Principal Symbols

a = amplitude of plane coherent wave
B = spatial-frequency bandwidth (cycles/mm)
D = circular aperture diameter
E_o = average exposure required over hologram area ($1/E_o$ = film sensitivity)
f = focal length of lens
g = $(2\pi/s\lambda)$
h = separation of adjacent apertures in screen
j = $\sqrt{-1}$
m = (s/f) = image magnification
N = number of outer apertures
P = storage density (bits/unit area)
p = $(2\pi/f\lambda)$
r = separation of outermost aperture from the reference aperture
s = separation of reconstructing and hologram planes
t_o = exposure time
T_A = amplitude transmission coefficient
W = Laser radiation power
U,V = rectangular co-ordinates referring to the reconstruction plane
X,Y = rectangular co-ordinates referring to the screen plane
x,y = rectangular co-ordinates referring to the recording plane
β = operating (bias) point on film transfer characteristic
λ = wavelength of radiation
τ = holographic efficiency

1. Introduction

Over the past few years there has been an intensive search in various laboratories[1-3] for new recording media and techniques capable of storing vast quantities of binary data with rapid access, fast transfer rates and sophisticated updating facilities, all (needless to say) at low cost. Many of these requirements and ideals are common to the problem of recording digital television signals in real-time, and a review of the possibilities (prior to 1969) was given in an earlier Research Report.[4] Subsequently, a growing interest has been shown in optical storage for binary data using holographic techniques, particularly in computer applications.[5] The concept which has emerged involves arrays of small holograms addressed by a laser beam, the reconstructed image so formed being read-out by a matrix of photosensors. Typically, for a read-only optical store, each hologram would be about 1 mm in diameter and contain 10^4 bits of information.

Redundancy is an intrinsic feature of holographic records which can be exploited, although not always easily. The general principle is that the information relating to each point of the original scene is spread[6] over the whole area of the hologram. Thus a small localised defect, e.g. a dust particle or scratch, on the record would have only a small effect on the reconstructed image. This holographic advantage of defect immunity, combined with the ruggedness achieved by binary coding, potentially offers a reliable and attractive system of digital data storage.

During 1970 various methods were suggested for applying these basic ideas of holographic storage to the real-time recording of digital television signals.[7] Although the systems proposed were elegant in concept, their practical implementation presented formidable problems in terms of existing technology; large arrays of fast-acting light valves and photo-sensors were required and such devices have yet to be developed to the stage of practicability. As an introductory step, an alternative system[8] was devised using micro-hologram arrays formed on conventional photographic film by a laser scanning arrangement. It was envisaged that each hologram would contain only a single word of eight or nine bits and have a diameter of approximately 30 μm (roughly equivalent to the diameter of a television picture element in conventional analogue recording on 35 mm cine-film). Although any hologram array format may be used, in principle, there would be a possible advantage in a line-by-line array, with a conventional aspect ratio, because a slight modification of the system might then permit a faint analogue version of the television picture to be recorded simultaneously. Such a picture, overlaid on the digital recording, could be useful for visual identification or editing.

A disadvantage of using micro-holograms is that, for a given packing density, a great deal, but not all, of the intrinsic holographic advantage of blemish immunity is sacrificed: this loss can be mitigated, however, by introducing redundancy in the binary coding. Moreover, the possibilities for word-error detection and concealment are increased. There are also two important practical advantages:—

(1) The number of fast-acting photosensors and light valves required is dramatically reduced, so that discrete transducers become practicable (and are, in fact, available).

(2) Because each micro-hologram contains only a few bits

of information, an on-axis reference beam[8] can be used (viz. Section 2.1) with the result that the hologram spatial-frequency bandwidth can be reduced by an order of magnitude, in fact to less than 200 cycles/mm.

The reduced bandwidth not only permits less critical physical tolerances during recording, and lower numerical lens apertures, but also less trouble arises from component surface dust and speckle effects. Another practical advantage is that higher-sensitivity photographic emulsions can be used, with a consequent reduction in the power of the laser source.

The work reported here is the initial phase of a feasibility study aimed at establishing a working system for recording digital television signals using hologram arrays. It is principally concerned with an investigation of low-frequency micro-holograms formed on several commercially-available photographic emulsions. The work has involved the design and construction of a laser-source test bench and a camera head, as well as the development of various measurement techniques. Measurements of resolution and transfer characteristics have been carried out on three different emulsions. These results, supported by data from other laboratories, are used to assess the maximum efficiency which can be expected and the relative importance of several fundamental parameters.

2. Theoretical considerations

2.1. Fourier transform holography

A typical arrangement for producing Fourier transform (F.T.) holograms is shown in Fig. 1. The transparency whose hologram is to be recorded is placed in the front focal plane (X,Y) of a lens, L. As indicated in Fig. 1, the transparency could be a thin screen, S, with a matrix of small holes in it representing 'bits' of information (presence or absence of a hole at a given point defining the binary state). A photographic plate or film, P, is placed in the rear focal plane (x,y) of the lens. During an exposure, the aperture screen is illuminated, as shown, by a beam of coherent radiation.* For those readers not familiar with lens systems, Fig. 1 might give the erroneous impression that P receives an actual image of the screen S. In fact, the light emerging from the lens is concentrated in a single, small spot at P.

The situation can be described more concisely in mathematical terms. If $F(X,Y)$ is the complex amplitude distribution of the radiation of the screen plane, and $G(x,y)$ is the corresponding distribution in the recording plane, then $G(x,y)$ is the Fourier transform of $F(X,Y)$, assuming the lens is perfectly corrected for geometrical aberrations. Hence, by adding simultaneously an inclined reference beam and then exposing the plate, a carrier-type hologram of the Fourier transform of the hole-pattern in the screen can be formed.

The proposals and experiments described later in this report are based on an alternative arrangement in which the reference beam is on-axis rather than inclined. An on-axis reference beam can be derived from a central aperture in the binary information screen. The new arrangement is shown in Fig. 2, where the central (reference) aperture of the screen is surrounded by only a small number of outer apertures. These latter could, for example, specify a single binary word. As will be shown later, the relative positions of the outer holes are carefully selected to avoid certain cross-talk effects appearing in the reconstruction. This

* The purpose of the aperture screen, when rear-illuminated, is to generate a set of coherent beams, sometimes called 'digit' beams. The insertion of an actual screen with apertures is not essential and other,[9] perhaps more suitable, methods of generating the coherent beams can be used. The treatment here only requires that the complex amplitude distribution of the radiation in the screen plane be specified.

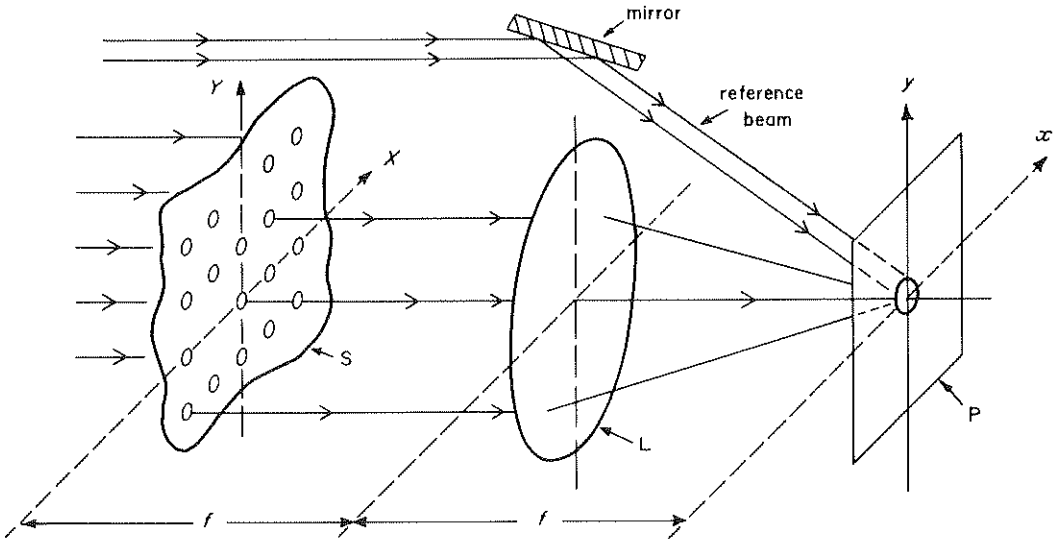

Fig. 1 - Typical arrangement for F.T. hologram recording

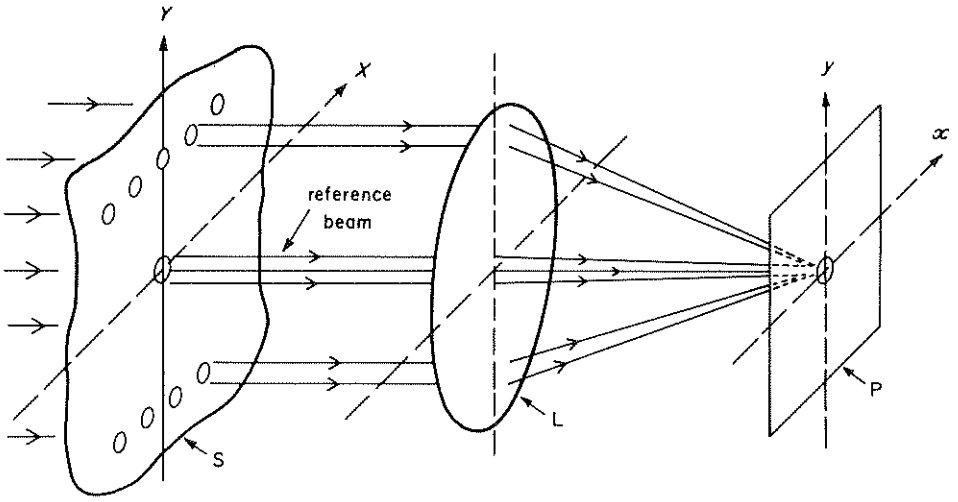

Fig. 2 - F.T. hologram recording using an on-axis reference beam

method of holography results in a baseband-type hologram having a relatively small spatial-frequency bandwidth.

2.2. Analysis for a multi-aperture screen

The principal features of the imaging, recording and reconstruction processes in F.T. holography can be gleaned from an analysis assuming an elementary, multi-aperture object screen.

2.2.1. Imaging

Let the object, or information screen, consist of an arbitrary array of N outer apertures located in the X,Y plane at the co-ordinates $X_1 Y_1$, $X_2 Y_2$ ... X_N, Y_N, as indicated in Fig. 3(*a*), and a central reference aperture at X_0, Y_0. All the apertures, including the reference, are assumed to be identical in size and form. During exposure, the apertures are illuminated by plane wave-fronts derived from a common coherent source, but with field amplitudes a_0, a_1 ... a_N at the respective apertures. Further let the function $F(X,Y)$ describe the spatial variation of the amplitude of the wave transmitted by each aperture.

It can be shown (using the displacement theorem of Fourier transforms) that the total amplitude distribution $A(x,y)$ in the recording plane (Fig. 3(*b*)) is given by

$$A(x,y) = G(x,y) \sum_{n=0}^{n=N} a_n \exp\left[-jp(X_n x + Y_n y)\right] \qquad (1)$$

where $G(x,y) = \iint_Z F(X,Y) \exp\left[-jp(Xx + Yy)\right] dX.dY.$

$p = (2\pi/f\lambda)$, f = focal length of lens λ = wavelength of radiation, Z = aperture zone, $F(X,Y) = 0$ outside Z, n = integer (n = 0 refers to the central reference aperture).

The spatial variation in the intensity of the radiation falling on a photographic plate, placed in the recording plane x,y, is equal to the square of the modulus of $A(x,y)$. Hence the exposure $E(x,y)$ is given by

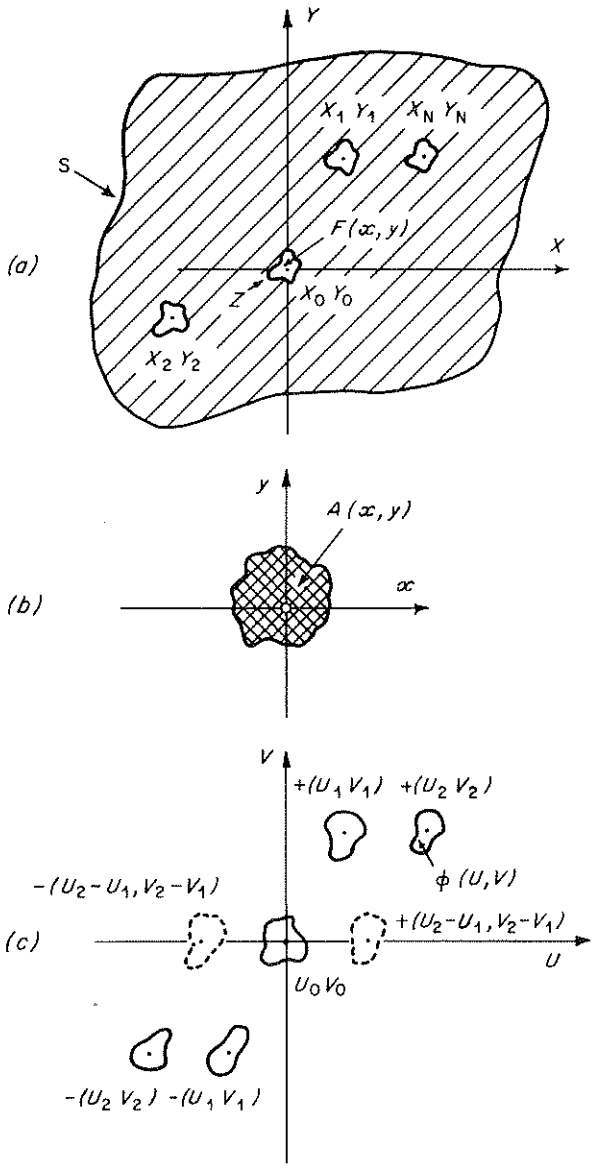

Fig. 3 - Analysis notation for a multi-aperture object screen

(*a*) Object screen with N outer apertures

(*b*) Amplitude distribution in Fourier Transform plane (hologram recording plane

(*c*) Reconstruction plane and image set for $N = 2$

$$E(x,y) = t_o A\ (x,y)\ A^*(x,y)$$

where t_o = exposure time and * denotes the complex conjugate. Thus, substituting from Equation (1)

$$E(x,y) = t_o|G(x,y)|^2 \left\{\sum_{n=0}^{n=N} a_n \exp\left[-jp(X_n x + Y_n y)\right]\right\}$$

$$\left\{\sum_{n=0}^{n=N} a^*_n \exp\left[jp(X_n x + Y_n Y)\right]\right\} \quad (2)$$

Equation (2) represents a complicated multi-beam interference pattern confined within the Fraunhofer diffraction pattern of a single aperture. The spatial-frequency bandwidth of the total pattern is determined by the greatest spacing between any two apertures in the screen, the focal length of lens and the wavelength of the radiation.

2.2.2. Recording

After exposure, the photographic plate or film is processed in the conventional manner to form a permanent hologram record. Alternatively, the silver-image can be subsequently bleached out to form a non-absorbing phase hologram. Ideally, using non-bleached holograms, the processed record should have an amplitude transmission factor, T_A, that is linearly related to the spatial variation of intensity during exposure.[10] That is

$$T_A(x,y) \propto (1/t_o)\, E(x,y) \quad (3)$$

Suppose we consider, however, using a negative hologram for the reconstruction, the negative having the transfer characteristic shown in Fig. 4(*a*). Here the development process is specified by the relation between the amplitude transmission factor T_A of the negative record and the normalised exposure. The dashed line represents the ideal linear case, while the full-line is typical of the relation achieved with high-resolution film emulsions. For comparison, Fig. 4(*b*) shows the same ideal and practical data replotted in the more conventional (H and D) form of optical density versus the logarithm of the exposure. Continuing the analysis, for the linear but negative case, we obtain instead of the proportionality (3)

$$T_A(x,y) = 1 - \beta[E(x,y)/E_o] \quad (4)$$

where E_o is the average exposure of the hologram, assumed to be adjusted such that the corresponding average value of T_A is $1-\beta$ (see Fig. 4(*a*)).† Two important general points concerning the hologram formation and the film exposure become apparent from Fig. 4 and Equation (4). These are

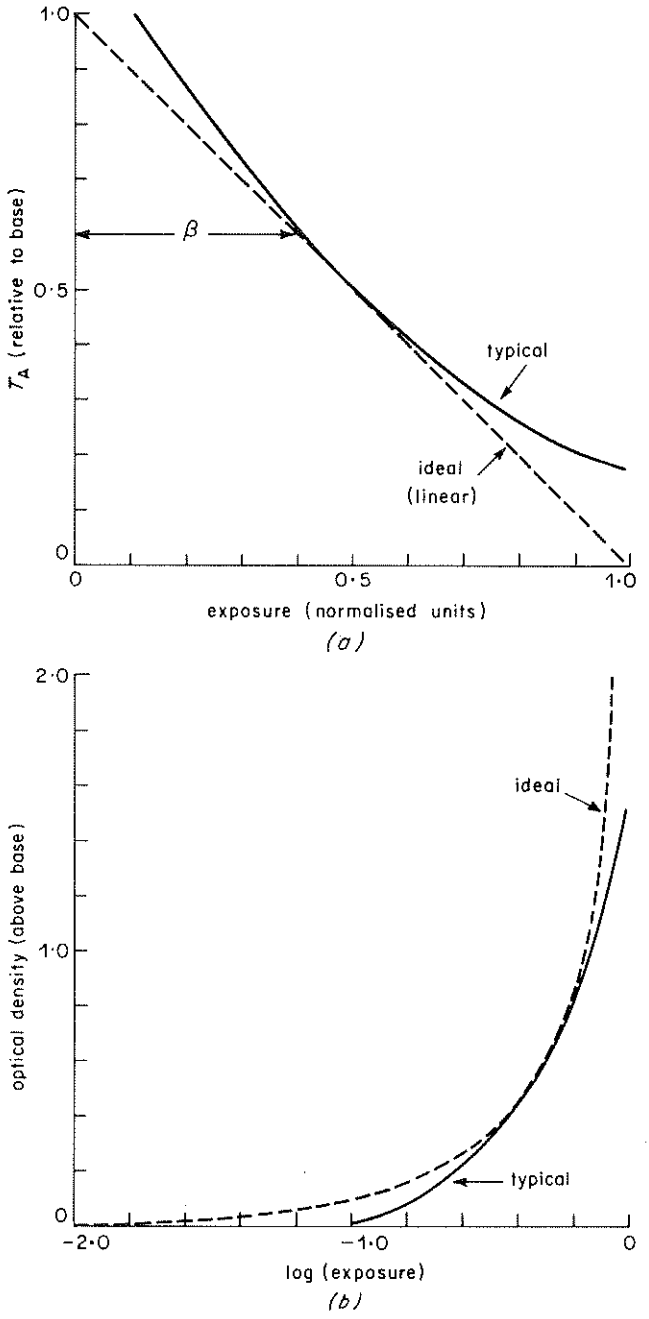

Fig. 4 - Negative film transfer characteristics for hologram recording

(*a*) Amplitude transmission factor T_A, as a function of relative exposure

(*b*) Conventional H and D plot of same data

(1) the point-to-point variations of intensity in the light forming the hologram should be confined to as small a range of intensity as possible in order to mitigate the effects of non-linearity. (Even in the ideal linear case we require that $E(x,y)$ be always less than $1/\beta$ times its average value.)

(2) there is not a great latitude in the bias point, β, for a practical system, without significantly changing the degree of transfer non-linearity. The actual tolerances are more profitably determined by experiment.

† β is an arbitrary operating (bias) point on the transfer characteristic of the recording emulsion and is selected by adjusting the average exposure.

(PH-105)

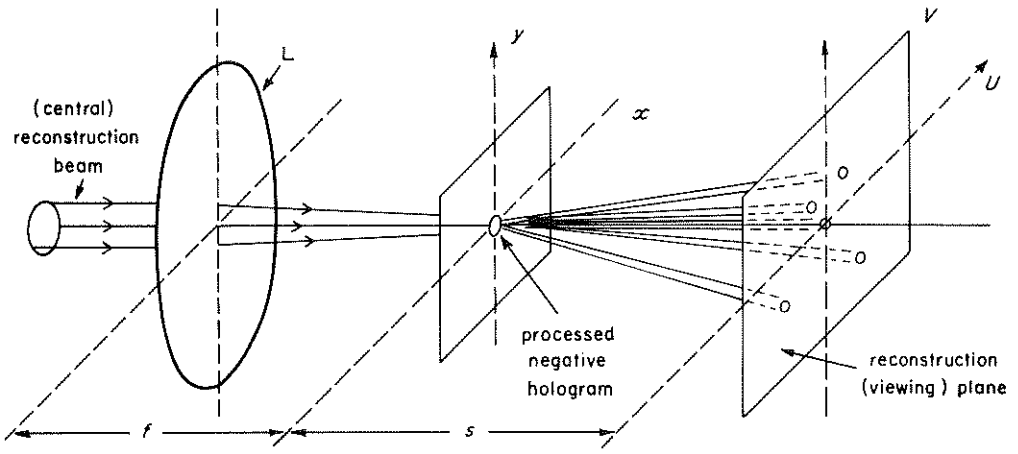

Fig. 5 - Reconstruction notation for F.T. hologram

2.2.3. Reconstruction

After processing, the negative hologram is replaced in its original position in the x,y plane and illuminated only by the reference beam (i.e. with only the central aperture of the object screen open) as shown in Fig. 5. The reconstructed image of the original outer apertures may be examined by placing a viewing screen (of ground glass say) in a plane (U,V) at a distance s from the hologram plane. It is assumed in the following that the distance s is very large compared with the hologram dimensions.

The spatial variation of amplitude of the light emerging from the negative hologram, $H(x,y)$ say, is

$$H(x,y) = T_A(x,y)\, G(x,y) \tag{5}$$

which, using Equation (4) becomes

$$H(x,y) = G(x,y) - (\beta/E_0)\, G(x,y)E(x,y) \tag{6}$$

Finally, the (far-field) diffraction pattern, $I(U,V)$ falling on the viewing screen S to form the reconstructed image in the U,V plane (see Fig. 5) is derived from the two-dimensional Fourier transform of $H(x,y)$. Thus

$$I(U,V) = \left| \int\int_{\infty} H(x,y) \exp\left[jg(xU + yV) \right] dx.dy \right|^2 \tag{7}$$

where $g = (2\pi/s\lambda)$.

Although Equations (5) and (7) formally describe the process for a multi-aperture object screen, the characteristics of the reconstructed image are more easily seen by looking at the individual terms obtained for a simple object screen with two outer apertures, say. Thus putting N=2 in Equation (2) and using Equations (6) and (7), one obtains:

$$\begin{aligned} I(U,V) = \Bigg| & F(U,V) - \beta\phi(U,V) \\ & - \frac{\beta a_0 a_1}{(a_0^2 + a_1^2 + a_2^2)}\, \phi(U \pm mX_1,\ V \pm mY_1) \\ & - \frac{\beta a_0 a_2}{(a_0^2 + a_1^2 + a_2^2)}\, \phi(U \pm mX_2,\ V \pm mY_2) \\ & - \frac{\beta a_1 a_2}{(a_0^2 + a_1^2 + a_2^2)}\, \phi[U \pm m(X_2 - X_1), \\ & \qquad V \pm m(Y_2 - Y_1)] \Bigg|^2 \end{aligned} \tag{8}$$

where $m = s/f$ (image magnification) and $\phi(U,V)$ is a normalised and scaled Fourier transform of the function $G(x,y)|G(x,y)|^2$. In fact, $\phi(U,V)$ can be regarded as a blurred version of the aperture function $F(U,V)$ $(\equiv F(X,Y)$ except for change of variable).

It may now be seen, from Equation (8), that the reconstruction of an object screen with N=2 consists of six separate light distributions having the form $\phi(U,V)$ and grouped into three sets of identical twin images. Each twin set has a different peak intensity. The images are located at the points $\pm(mX_1\ mY_1)$, $\pm(mX_2,\ mY_2)$ and $\pm[m(X_2 - X_1),\ m(Y_2 - Y_1)]$ respectively. In addition a different distribution, $F(U,V) - \beta\phi(U,V)$, having the largest peak intensity, occurs on the optical axis, i.e. at $U = 0$, $V = 0$.

The reconstructed version of a 2-aperture screen (plus the central reference aperture) is shown in Fig. 3(*c*). In addition to those images having the same geometrical disposition as the original apertures, there is a duplicate set mirrored in the opposite quadrant, plus a spurious pair of images; these latter images are symmetrically disposed about the origin and are separated from the origin by an amount equal (or proportional) to the original separation of the screen apertures.

2.3. Hologram efficiency

Small photo-detectors placed in the reconstruction plane at the corresponding geometrical positions of the N

original screen apertures can be used to indicate whether or not a particular aperture was 'open' during the exposure of the spot hologram. This provides a means of recovering the original binary word in electrical form.

Now, if the (blurred) images in the reconstruction are sufficiently well separated, the analysis in Section 2.2 above suggests that the intensity distribution of the nth wanted image in the reconstruction is given by an expression of the form

$$\left[\beta a_n a_o \left(\sum_{n=0}^{n=N} a_n^2\right)^{-1}\right] \left|\phi(U,V)\right|^2$$

The first factor in the above expression indicates the theoretical efficiency of the process, while the last factor describes the spatial variation of image intensity. Both factors are important in relation to the maximum storage capacity of the individual holograms and the signal-to-interference ratio of the system.

The holographic efficiency, τ, can be defined as the ratio of the average power of the radiation forming a wanted image to that of the reconstructing beam. For a non-bleached hologram, having a transfer characteristic specified by Equation (4) and with perfect resolution characteristics, the hologram efficiency for the nth aperture of a multi-aperture screen is

$$\tau = \left[\beta a_n a_o \left(\sum_{n=0}^{n=N} a_n^2\right)^{-1}\right] \qquad (9)$$

where it is assumed that the N outer apertures and the reference aperture have identical size and form. If it is assumed that all the outer apertures were illuminated with equal intensity during the exposure, Equation (9) reduces to

$$\tau = \frac{\beta^2 (a/a_o)^2}{[1 + N(a/a_o)^2]^2} \qquad (10)$$

where a^2 = illumination intensity of the N outer apertures.

Thus, in this case, the holographic efficiency depends on

(i) the bias-point, β, on the transfer characteristic,
(ii) the number N of outer (signal) apertures,
(iii) the ratio $(a/a_o)^2$, which is the ratio of the illumination intensities of the outer apertures to that of the reference aperture.

It is easily shown that the maximum value of τ in Equation (10) is obtained when $N(a/a_o)^2 = 1$, i.e. when the sum of the illumination intensities of the N outer apertures equals that of the reference aperture. Thus, from Equation (10)

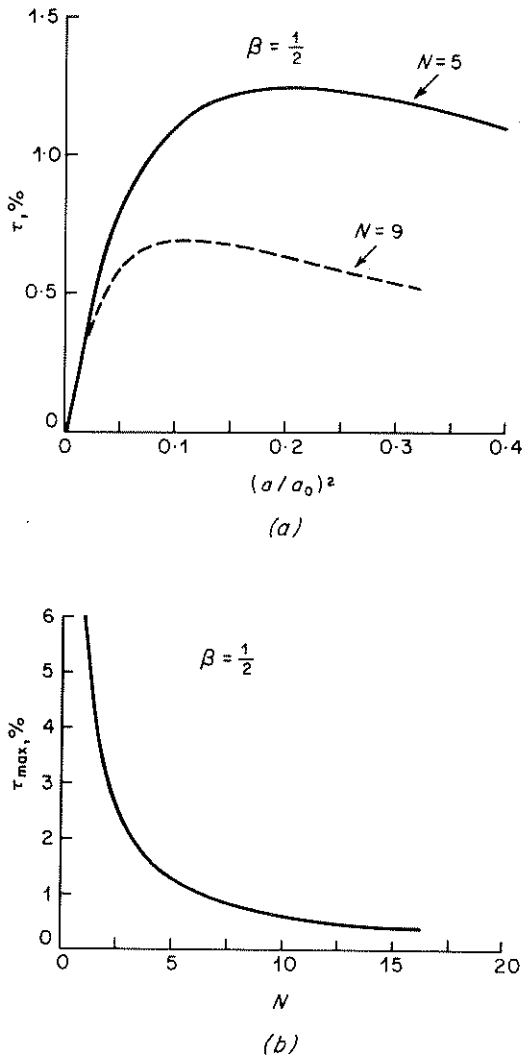

Fig. 6 - Theoretical efficiency for a non-bleached hologram of a binary screen with N identical outer apertures

(*a*) Variation of efficiency with ratio of outer-to-reference aperture illumination for $N = 5$ and $N = 9$

(*b*) Maximum efficiency of process as a function of number of outer apertures

$$\tau_{max} = \frac{\beta^2}{4N} \qquad (11)$$

Fig. 6(*a*) shows the variation of the holographic efficiency, τ, with $(a/a_o)^2$ for N=5 and for N=9, as given by Equation (10) with β=½. Fig. 6(*b*) shows the inverse proportionality of τ_{max} with N, as given by Equation (11), again with β=½.

The modulation transfer functions or resolution characteristics of actual photographic emulsions tend to droop with increasing spatial frequency, and this reduces the holographic efficiency of the process. Equalisation of the holographic efficiencies for the individual apertures can be achieved, however, by a compensatory adjustment of their respective illumination intensities at the time of exposure.

Variations in the holographic efficiency can also be expected with deviations from linearity in the negative transfer characteristic and from changes in the bias point.

Greater efficiencies are possible by bleaching the holograms after development to produce non-absorbing phase holograms, although some adverse features have been reported.[11]

2.4. Digital storage capacity

Using the concept that each separate aperture in the object screen corresponds to one 'bit' of information, the storage per hologram spot is simply equal to the number N of outer apertures. If Z is the effective area of the reference aperture, the corresponding area of the hologram spot is proportional to $f^2\lambda^2 Z^{-1}$ where, as previously, f is the focal length of the lens and λ is the wavelength of the light.† Hence, thinking in terms of a two-dimensional array of small holograms, the storage density P(bits/unit area) is

$$P = \frac{k_1{}^2 NZ}{f^2\lambda^2} \qquad (12)$$

where k_1 is a coefficient determined by the closeness with which the hologram can be packed in the array without producing significant cross-talk between neighbouring holograms. The value of k_1 is best determined by experiment, and is expected to be less than unity.

The achievable storage density must, however, be weighed against other basic criteria such as the overall error-rate in the reconstituted binary signal.

The concept of micro-hologram arrays of single binary words leads to a holographic system of low spatial-bandwidth because the low number of bits per hologram allows an on-axis reference beam to be used. In this case, the system bandwidth is given by $(r/f\lambda)$, where r is the separation in the plane of the aperture screen of the outermost aperture from the reference aperture.* Suppose we have an aperture screen representing a 9-bit word arranged as shown in Fig. 7(*a*). The circular apertures lie along two rows, $Y = 2h$ and $Y = -3h$ respectively. The apertures have a diameter D and are spaced h apart ($h > D$). It can be easily seen that, with this design, the spurious images arising in the reconstruction, due to a simultaneous exposure of all the apertures, lie clear of the wanted set of images. Moreover, any second order diffraction images arising from transfer non-linearity will also lie clear of the wanted set of images. In an alternative design, the apertures lie on circular arcs of radii $2h$ and $3h$ respectively as shown in Fig. 7(*b*). For this particular aperture screen arrangement, r is equal to $3h$ and therefore the system spatial frequency bandwidth is $(3h/f\lambda)$. In order to avoid significant cross-talk between neighbouring images in the reconstruction the screen aperture diameters must be somewhat less than their

† This relationship arises due to diffraction at the aperture.

* Two parallel coherent beams separated by a distance r and brought to a focus by a lens of focal length, f, produce a sinusoidal variation of intensity in the focal plane which has a (maximum) spatial frequency variation equal to $(r/f\lambda)$, where λ = wavelength of the radiation.

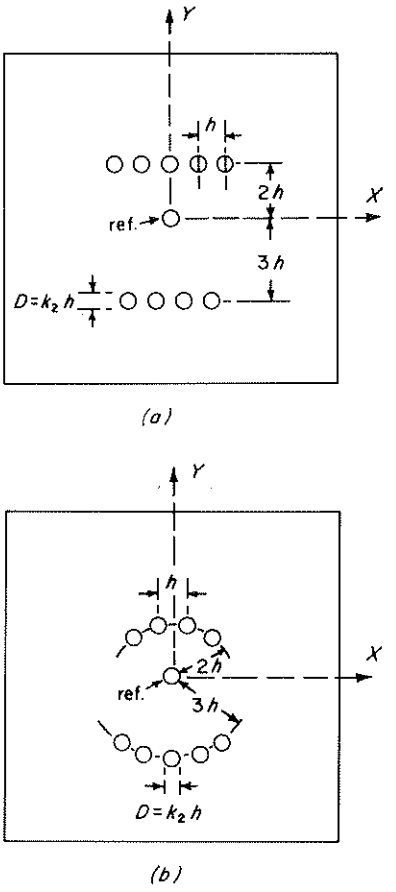

Fig. 7 - Binary aperture screens for low-bandwidth F.T. holograms

(*a*) Nine-bit screen arrangement (*b*) Alternative design

spacing, i.e. $D = k_2 h$ where k_2 is a coefficient less than unity. Thus, in terms of the spatial-frequency bandwidth B, the storage density using the nine-aperture screen shown in Fig. 7(*b*) becomes (substituting for $f\lambda$, and NZ in Equation (12)

$$P = (k_1 k_2 B)^2 \qquad (13)$$

As a numerical example, setting $k_1 = k_2 = 1/\sqrt{2}$ (which is about the practical limit) and B = 200 cycles/mm, the storage density is 10^4 bits/mm^2 (10^6 bits/cm^2). At this density, a high-quality digital television recording of a scene would occupy an area of film equal to that of a conventional 35 mm cine-film frame.

An estimate of the minimum spacing of the apertures in the object screen, i.e. of the value of k_2 in Equation (13), can be obtained by calculating the reconstructed image profile for a single aperture. It has already been mentioned (Section 2.2.3) that the reconstructed image will be a blurred version of the original aperture. The image profile ($\phi(U,V)$ in Equation (8)) calculated for the case of a circular aperture is shown in Fig. 8. It will be seen that the profile spreads to approximately twice the original aperture diameter, so that for no interference between adjacent images the minimum aperture separation is also this value, i.e. k_2 = ½. However, some overlap of the images is per-

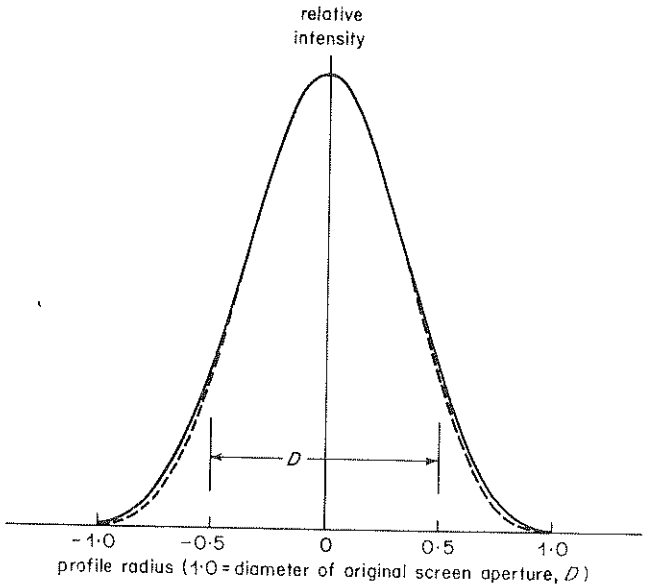

Fig. 8 - Calculated intensity profile (principal section) of reconstructed image

——— linear transfer characteristic
– – – – typical transfer characteristic

missible is practice, especially if only the core of the image is used for binary on/off sensing.

Although the salient features of the system can be deduced by considering circular apertures uniformly illuminated, there are alternative variations which could lead to less crosstalk, not only between adjacent reconstructed images, but also between adjacent holograms in the recorded array. For example, by tailoring the radial variation of amplitude and phase of the radiation leaving the primary screen apertures (i.e. by 'apodisation') the hologram spot could be more uniformly exposed. This would be especially beneficial because of the small latitude for correct exposure. However, a full investigation of these possible refinements is beyond the scope of this report.

2.5. Laser power requirements

In this section, the factors which control the input and output information transfer rates are considered in general terms. The transfer rate required for real-time television recording and replay in digital form is of the order of 10^8 bits per second, and it is this very high rate which really stretches the existing technology with regard to suitable transducers.

2.5.1. Writing

The basic factors which determine the potential transfer rate in recording hologram arrays on photographic film are

(i) sensitivity of the film
(ii) modulation transfer function (MTF) of the film
(iii) optical efficiency of the system
(iv) laser radiation power.

It is well known that the first two factors are somewhat incompatible in the sense that high sensitivity and high resolution characteristics do not go together. Many of the emulsions used for conventional holography have very high resolution capabilities (> 2000 cycles/mm) but are also exceedingly slow.

The third factor, optical efficiency, depends on the particular system of recording and scanning devised. It might be thought that high efficiencies could be obtained easily with coherent laser beams, but this is not so, especially if sophisticated beam-deflection devices and fast modulators are required. Overall optical efficiencies greater than about 20% could be difficult to achieve, at least in the early stages of development.

The laser radiation power, W (milliwatts), required for real-time recording at an input transfer rate of I (bits/sec) is given by

$$W = \frac{IE_o}{\mu P} \times 10^{-3} \quad \text{(mw)} \qquad (14)$$

where μ is the overall optical efficiency of the system, P is the information packing density (bits/cm^2) and $(1/E_o)$ is the reciprocal exposure or sensitivity of the recording film in $(\mu J/cm^2)^{-1}$.

Fig. 9 shows a plot of laser power W as a function of packing density P, with film sensitivity $(1/E_o)$ as a parameter; a transfer rate of 100 Megabits/sec and an optical efficiency μ of 10% have been assumed. The film sensitivity values cover the range of commercially available holographic emulsions. For micro-hologram arrays, the packing density is proportional to the square of the system bandwidth (see Equation (13)), and the modulation transfer factor of the recording film must be adequate at the maximum spatial frequency required. Furthermore, on sub-

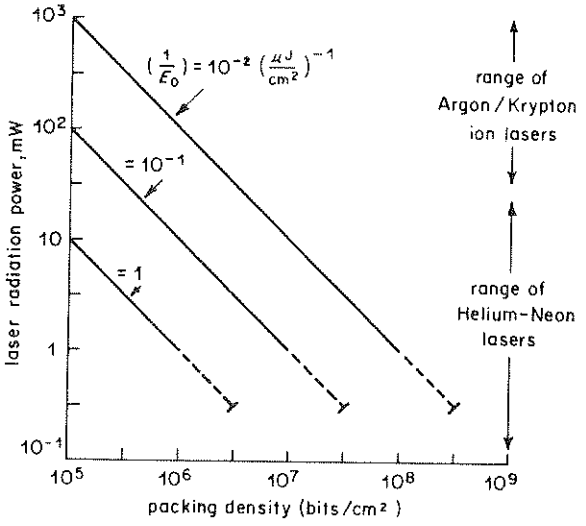

Fig. 9 - Laser power required for holographic recording as a function of packing density with film sensitivity $(1/E_o)$ as parameter

Optical efficiency = 10%; recording rate = 10^8 bits/sec.

stituting Equation (13) in Equation (14) and then re-arranging, the product $(1/E_0)B^2$ occurs in the denominator of the expression for the laser power. Now, for a range of recording films the product of the sensitivity and the square of the spatial frequency bandwidth tends to be roughly constant, and this is the reason for the limit marks on the plot shown in Fig. 9. The point emphasised here is that the slower but higher resolution films are necessary for television recording at very high packing densities.

Providing that an optical efficiency in the recording arrangement greater than 10% can be achieved, it would appear that low-power gas lasers (5 to 10 milliwatts) would be suitable for a television recording system using micro-hologram arrays.

2.5.2. Reading

The principal criterion in relation to the laser power required for the reconstruction or read-out system is that the overall error-rate is not significantly increased by photon noise in the reading beam. The limiting values of signal-to-noise ratio as a function of radiation power at λ = 632·8 mm (He-Ne) incident on a photodetector are shown in Fig. 10, for various values of detector bandwidth. A photodetector quantum efficiency of 5% has been assumed (typical value for an S20 photo-cathode at this wavelength).

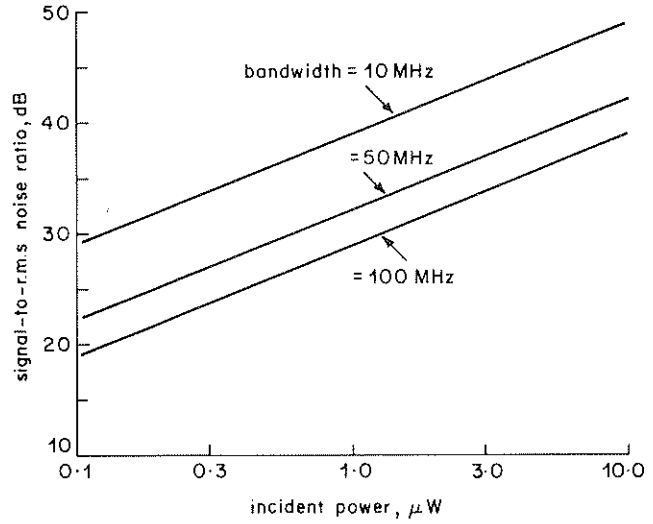

Fig. 10 - Limiting signal-to-noise ratios for a photo-detector (quantum efficiency = 5%) as a function of incident power with detector bandwidth as parameter

The reconstruction efficiency to be expected with non-bleached holograms was discussed earlier (Section 2.3), and efficiency values between 0·1% and 0·5% are typical. If we regard a limiting signal-to-noise ratio (due to photon noise) of 40 dB with a detector bandwidth of 50 MHz as adequate, then we require an incident radiant power of at least 6 μW on each detector (5% quantum efficiency). The required radiation power incident on each hologram, therefore, falls in the range 1·2 mW to 6 mW in this example. Assuming an optical efficiency in the read-out apparatus of 20%, the laser power required is at least 6 mW, which is commensurate with that required for writing.

The laser power required for reading could be significantly reduced by using a photodetector with a high quantum efficiency at λ = 632·8 nm, e.g. a fast silicon photo-diode having a quantum efficiency of 60%.

3. Film sample measurements

Some basic measurements were made on several commercially-available film emulsions which were thought to be potentially useful for low-frequency micro-hologram recording. It appeared originally, from manufacturers' data, that there was a considerable range of film emulsions available. However, the actual selection available off-the-shelf was limited, largely due to recent 'rationalisation' of these materials by the principal manufacturers. In the event, four film stocks (Ilford Micro-Neg Pan; Agfa Copex Pan Rapid; Kodak micro-file 5669; Agfa Scientia 10E 75) were investigated experimentally. After the initial measurements it was found that Agfa Copex Pan Rapid was similar to Ilford Micro-Neg Pan and, therefore, was not included in the subsequent experiments.

3.1. Transfer characteristic and sensitivity

The transfer characteristics were measured by exposing the emulsions through a calibrated neutral-density step wedge to a uniform beam of laser radiation (He-Ne laser at λ = 632·8 nm). The results are shown in Fig. 11, where the amplitude transmission coefficient is plotted as a function of exposure (log scale). Throughout the work the development conditions have been held constant; 4 mins. in Kodak D.19 (or Ilford Phentrace) at 20°C with nitrogen bubble-burst agitation every 30 seconds. The exposure times were in the region of 40 ms, i.e. near the maximum photometric efficiency.

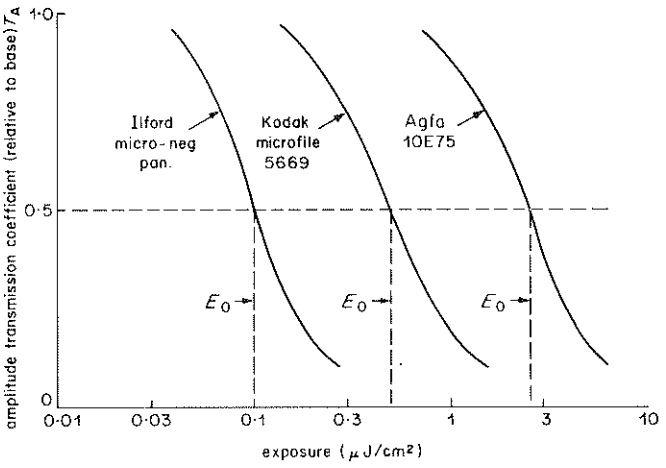

Fig. 11 - Transfer characteristics of film emulsions; amplitude transmission T_A versus exposure in $\mu J/cm^2$ (log scale)

Sensitivity, for this application, may be defined as the reciprocal of the exposure required to reach a given point on the transfer characteristic. A convenient point is where the amplitude transmission coefficient equals ½, for which an exposure E_0 is required; these bias points are shown on the curves in Fig. 11.

The results shown in Fig. 11 refer to relatively long exposures, and it is well known that for much longer or much shorter exposure times reciprocity failure occurs; the effect is to diminish the photometric efficiency of the emulsion. Measurements made on the film samples indicated a decrease in effective sensitivity by a factor of $^1/_3$ for an exposure time of about 100 microseconds (x3 reciprocity factor). The experience of other laboratories* working on pulsed holography is that for exposure times below about 10 microseconds no further reciprocity failure occurs. For exposures in the nanosecond range, the photometric efficiency of a holographic-type emulsion is expected to be not less than (¼) of its maximum value.

3.2. Modulation transfer function

The M.T.F. of film emulsions at spatial frequencies greater than 100 cycles/mm is not easily measured by conventional methods, e.g. by scanning line-spread functions or other recorded image patterns. A more satisfactory approach is to record a sine-wave intensity pattern, directly generated by two interfering beams of coherent light, and then to measure the diffraction efficiency of the processed record, again using a coherent light beam.

Fig. 12(*a*) shows the arrangement used to generate sets of interference fringes of various (fixed) spatial frequencies, with control of modulation-depth. Fig. 12(*b*) indicates the method used for measuring the diffraction efficiency of the test recordings.

The principal results obtained are shown in Fig. 13, where each curve plotted is the variation of the intensity of the first-order diffraction component (n_1) as a function of the zero-order intensity (n_0), for the stated spatial frequency and for 100% modulation depth of the interference fringes during exposure. The intensities are expressed as a percentage of the incident intensity, where the latter is

* N.P.L., Kodak Laboratories.

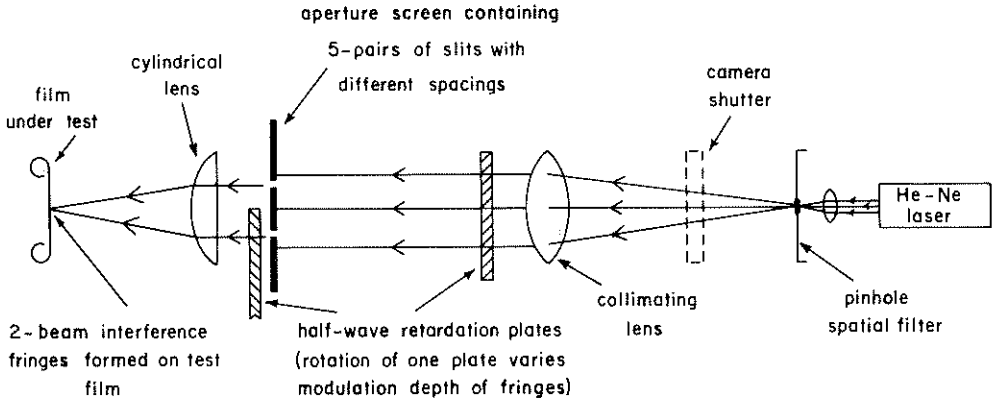

(a)

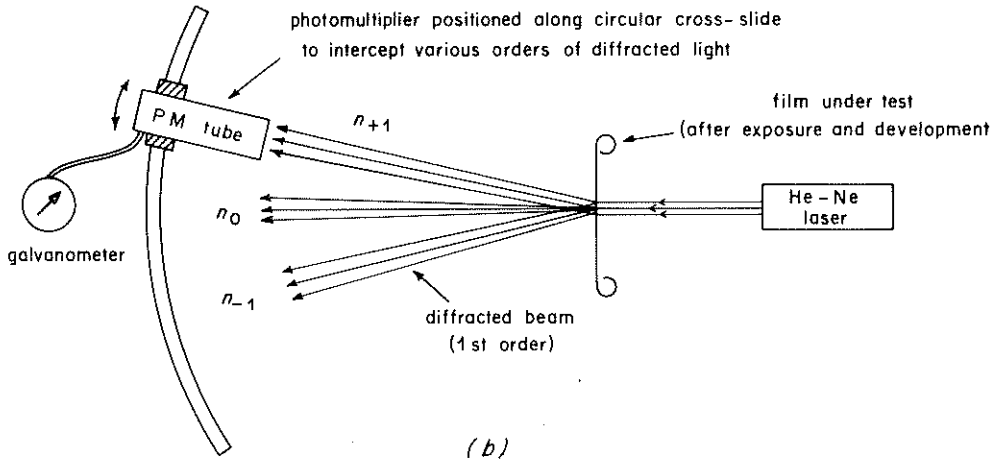

(b)

Fig. 12 - Arrangement used to measure effective modulation transfer functions film emulsions up to 200 cycles/mm
(*a*) Generation of sinusoidal intensity patterns on film sample (*b*) Measurement of diffraction efficiency

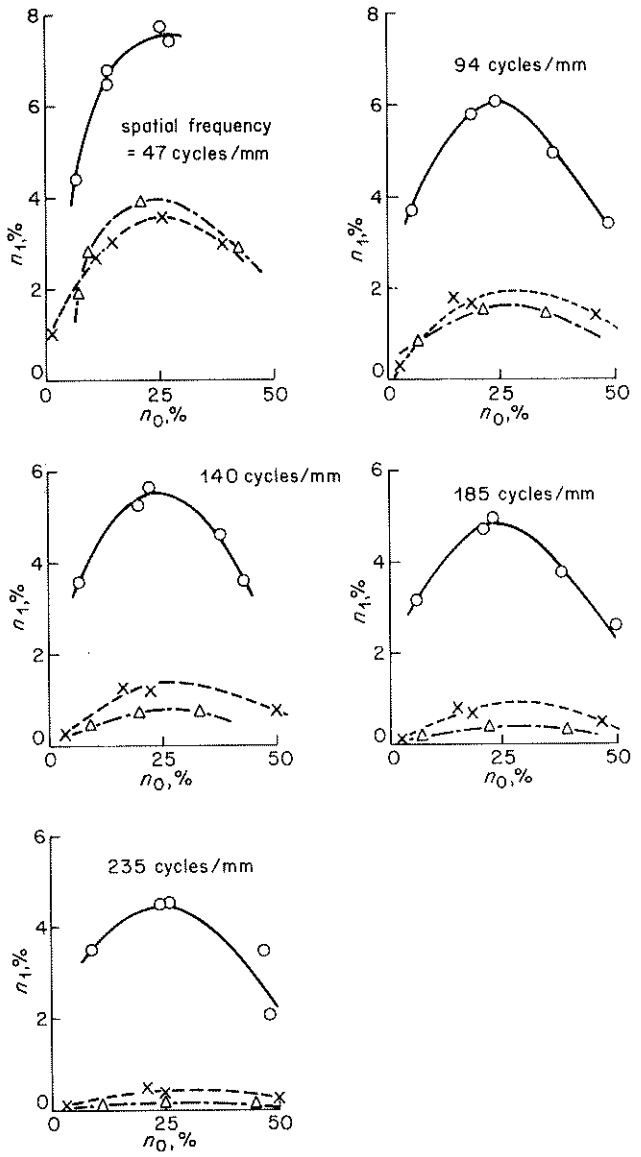

Fig. 13 - Measured diffraction efficiency of test samples: 1st order component n_1 as a function of the undiffracted (zero-order) component n_0, for various spatial frequencies

○——○ Agfa 10E 75 x----x Kodak Microfile 5669

△—·—△ Ilford Micro-Neg Pan

taken to be the transmitted intensity of the incident light in the unexposed region of the record. All results were obtained using He-Ne laser radiation at λ = 632·8 nm.

A derived set of curves, which are equivalent to the M.T.F.'s for the films tested, are shown in Fig. 14, where the maximum first order diffraction intensity is plotted as a function of spatial frequency for each film type. The measured intensities are shown normalised to the theoretical diffraction intensity for a perfect sine-wave amplitude grating with 100% modulation depth. Also marked on the figure is the theoretical level for the first-order component of a square-wave grating.

It will be noticed that, for one film type (Agfa 10E 75), the diffraction efficiency at low spatial frequencies exceeds the theoretical level for a sine-wave grating. This reflects the fact that the amplitude transmission characteristic of the film has only a limited region of linearity, so that the extreme excursions of exposure occuring with a high modulation depth are 'crushed', resulting in a recorded pattern which tends to have a square-wave form.

There are several other conclusions which can be drawn from these diffraction measurements:

(1) The optimum diffraction efficiency occurs for a zero-order intensity in the region of 25%. (See Fig. 13). This is equivalent to an amplitude transmission coefficient Ta = 0·5, which is the region of the transfer characteristic that is most linear and has the greatest slope (Fig. 11). This is clearly an optimum bias point for holographic applications where minimum distortion and maximum efficiency are required.

(2) The range of zero-order intensities for which the diffraction efficiency is greater than 50% of its maximum value, irrespective of spatial frequency, appears to be from 5% to 50% approximately. Taking this range as a practical tolerance for holographic applications, the corresponding latitude for exposure is from $0{\cdot}3E_o$ to $1{\cdot}75E_o$, where E_o is the optimum exposure.

(3) Although the two most sensitive films have some response at spatial frequencies above 200 cycles/mm,

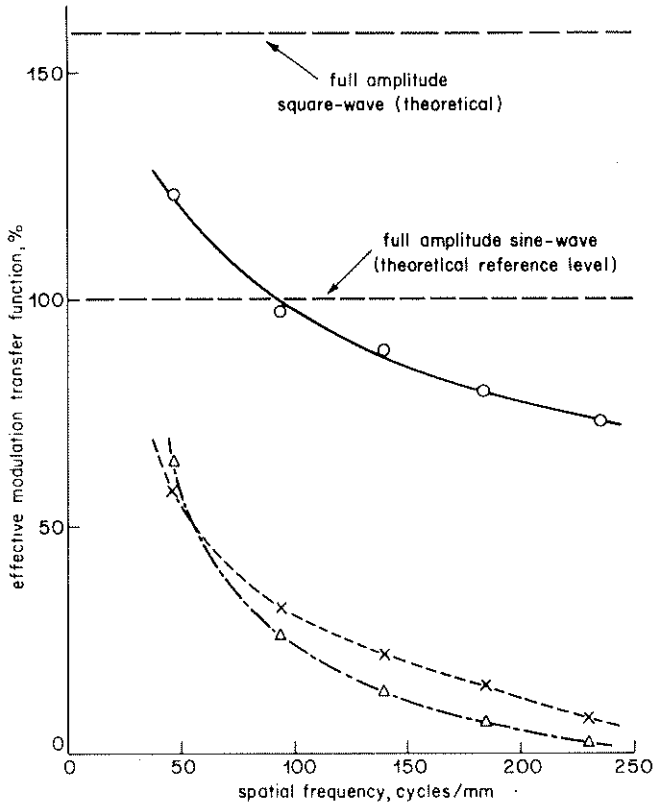

Fig. 14 - Effective modulation transfer functions of film samples

○——○ Agfa 10E 75 x--x Kodak Microfile 5669

△—·—△ Ilford Micro-Neg Pan

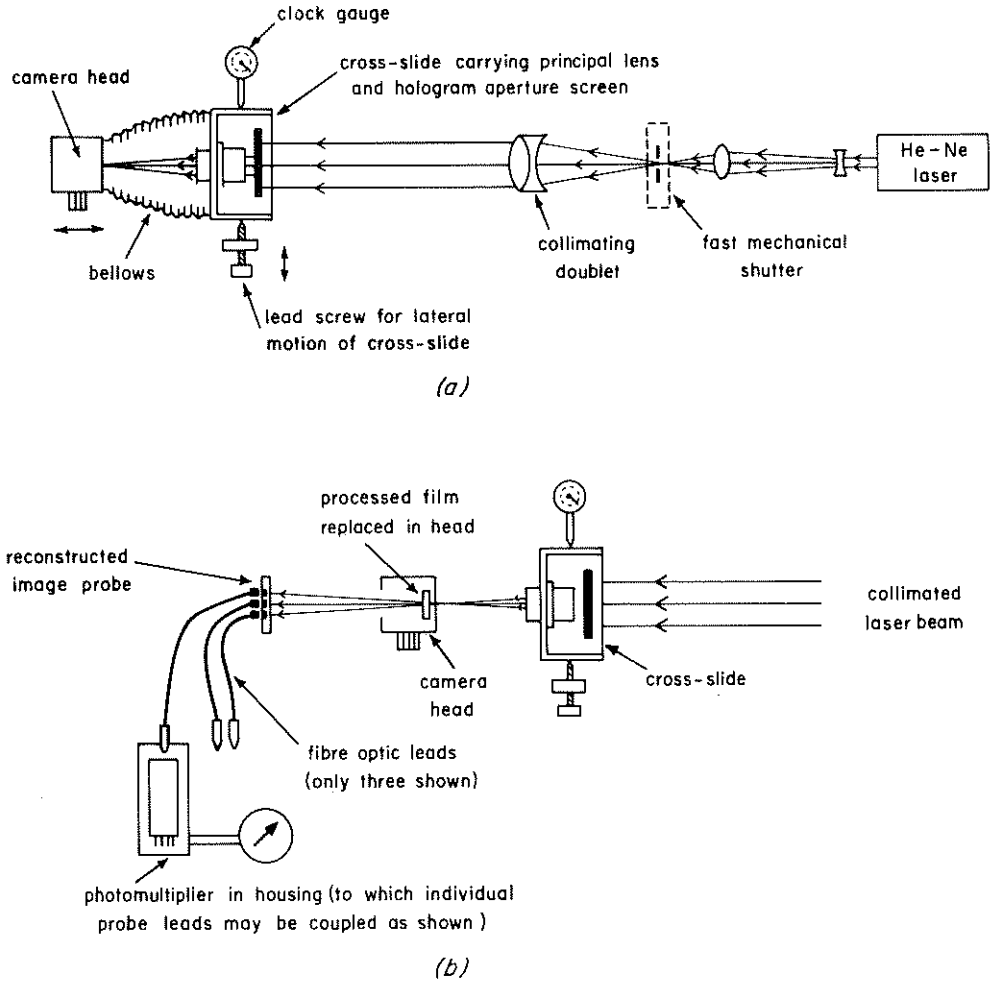

Fig. 15 - Arrangements for exposing and measuring micro-holograms
(*a*) Recording the holograms (*b*) Assessing the reconstructed image

the diffraction efficiency begins to droop severely at much lower spatial frequencies. Their effective M.T.F.'s compare most unfavourably with that of the slowest (least sensitive) film.

4. Micro-hologram experiments

An arrangement for exposing film samples to produce low-frequency micro-holograms was constructed as outlined in Fig. 15(*a*). A fast mechanical shutter was used to obtain exposures in the range 50 to 500 microseconds. The hologram aperture screen and principal lens were mounted on a transverse slide controlled by a screw thread. Hence, by successive lateral displacements and exposures, rows of spot holograms could be produced.

In order to measure the reconstruction properties of the test holograms, an extension to the recording apparatus was constructed as shown in Fig. 15(*b*). The outer holes in the aperture screen were blanked off and the processed film sample replaced and registered in the film holder. A search probe, consisting of an array of small (1 mm dia.) fibre-optic light guides, was placed about 10 cms behind the film holder. The guides were arranged to have the same geometrical disposition as the wanted set of reconstructed images (including the central zero-order component for reference). The relative image intensities were measured by coupling the free end of each guide in turn to a photomultiplier.

For many of the tests, object-screens were constructed based on the designs described earlier (Section 2.4). The collimated light incident on the object-screen was plane-polarised, so that by sliding a piece of half-wave retardation plate (with its axes suitably orientated) over an aperture the polarisation could be rotated through 90°. In this condition, no interference can take place in the hologram plane between light from that particular aperture and that from the reference aperture. Hence, the aperture is effectively switched off and it will not appear in the subsequent reconstruction of the hologram.[8] Moreover, the switching effect is accomplished without altering the average exposure, which would not be the case if the apertures were simply blanked off.

4.1. 5-bit holograms (40 μm dia.)

Initially, 5-bit holograms (i.e. 5 outer apertures in the object screen) were produced having an effective diameter

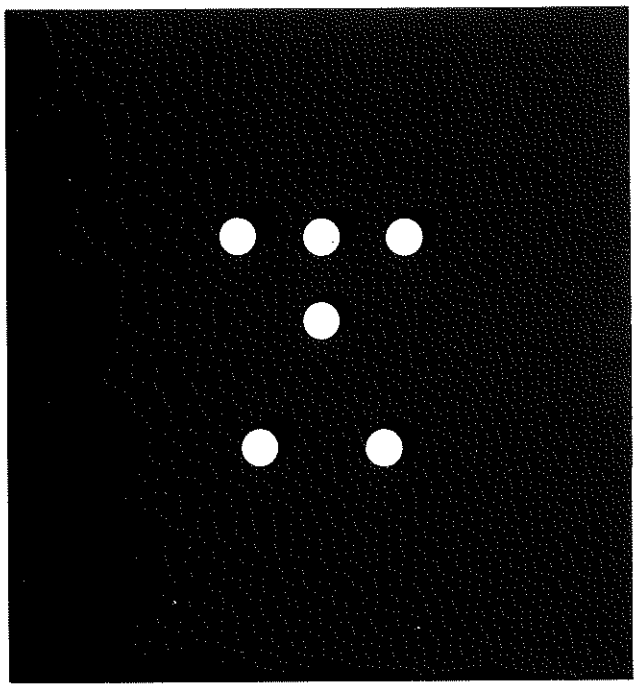

(*a*)

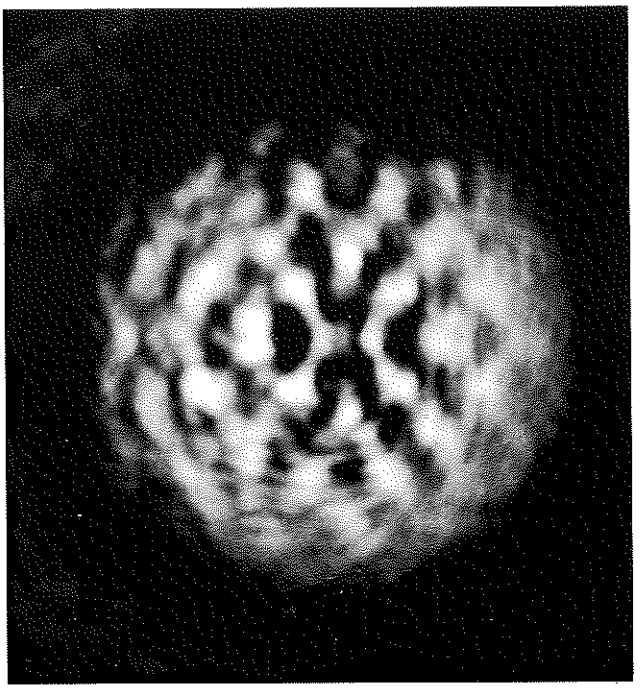

(*b*)

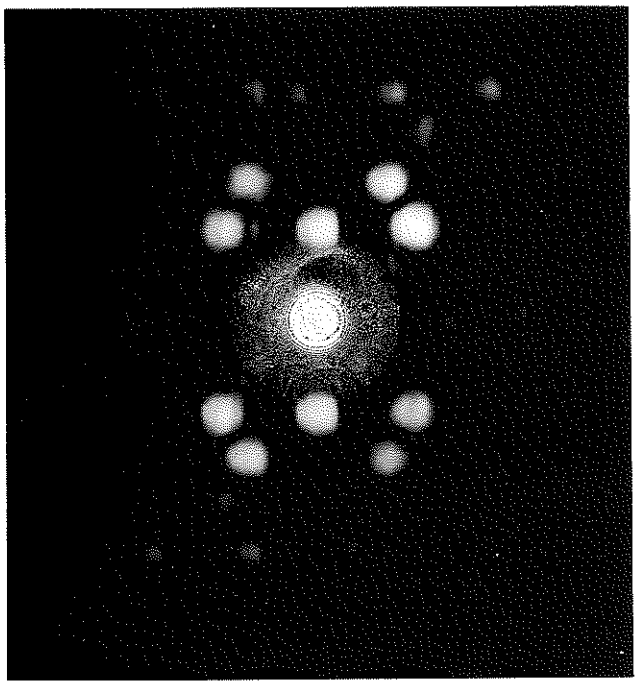

(*c*)

Fig. 16 - Formation and reconstruction photographs of a 5-bit hologram (40 μm dia.)

(*a*) Transmission pattern of original object screen

(*b*) The micro-hologram intensity pattern

(*c*) The reconstructed image pattern (showing image blurring and extraneous images)

of 40 μm and a maximum spatial frequency of 120 cycles/mm. Fig. 16(*a*) is a transmission photograph of the original screen pattern, Fig. 16(*b*) is a microphotograph of the actual F.T. hologram while Fig. 16(*c*) is a photograph of the reconstructed image showing the expected image blurring and extraneous images (all but the wanted set of images would normally be masked off).

Similar micro-holograms were formed on each of the film stocks and photo-electric measurements were made of their diffraction efficiency. The measured results are summarised in Table 1 where, for comparison, the last column shows the theoretical maximum expected for each emulsion type.

The next stage was to form a row of 5-bit holograms, spaced 40 μm apart; starting with no outer apertures 'on' for the first hologram, each subsequent hologram had one

TABLE 1
5-bit, 40 μm diameter holograms

Emulsion type	M.T.F. @ 100 cycles per mm	Hologram spacing μm	Diffraction Efficiency % (average per bit)	
			Measured	Theoretical (Max.)
Agfa 10E 75	0·98	40	0·72	1·22
Kodak Microfile 5669	0·3	40	0·16	0·37
Ilford Micro-Neg Pan	0·24	40	0·2	0·3

more aperture 'open' than its predecessor. During reconstruction, the incident beam was manually scanned over the row of holograms and the corresponding variation of light intensity in each of the (fixed) image locations was determined. These results are shown plotted in Fig. 17(*a*). With respect to the arbitrary intensity threshold marked on the figure, it will be noted that threshold-to-background intensity ratio is generally better than 10 : 1 (20 dB); part of the background light measured was, in fact, due to the veiling glare introduced by the principal lens and is not the result of image crosstalk or noise. If the electrical outputs of five photodetectors, optically coupled to each image location respectively, had been connected to simple level comparator circuits, the binary quantised outputs would be approximately those shown in Fig. 17(*b*).

4.2. 9-bit holograms (30 μm dia.)

The first attempts to form 9-bit holograms with a diameter of 30 μm, while still maintaining a spatial-frequency bandwidth of 120 cycles/mm, were unsuccessful due to inter-bit crosstalk; the object-screen apertures were too close to each other in relation to the diameter of the reference aperture. Better reconstruction imagery was

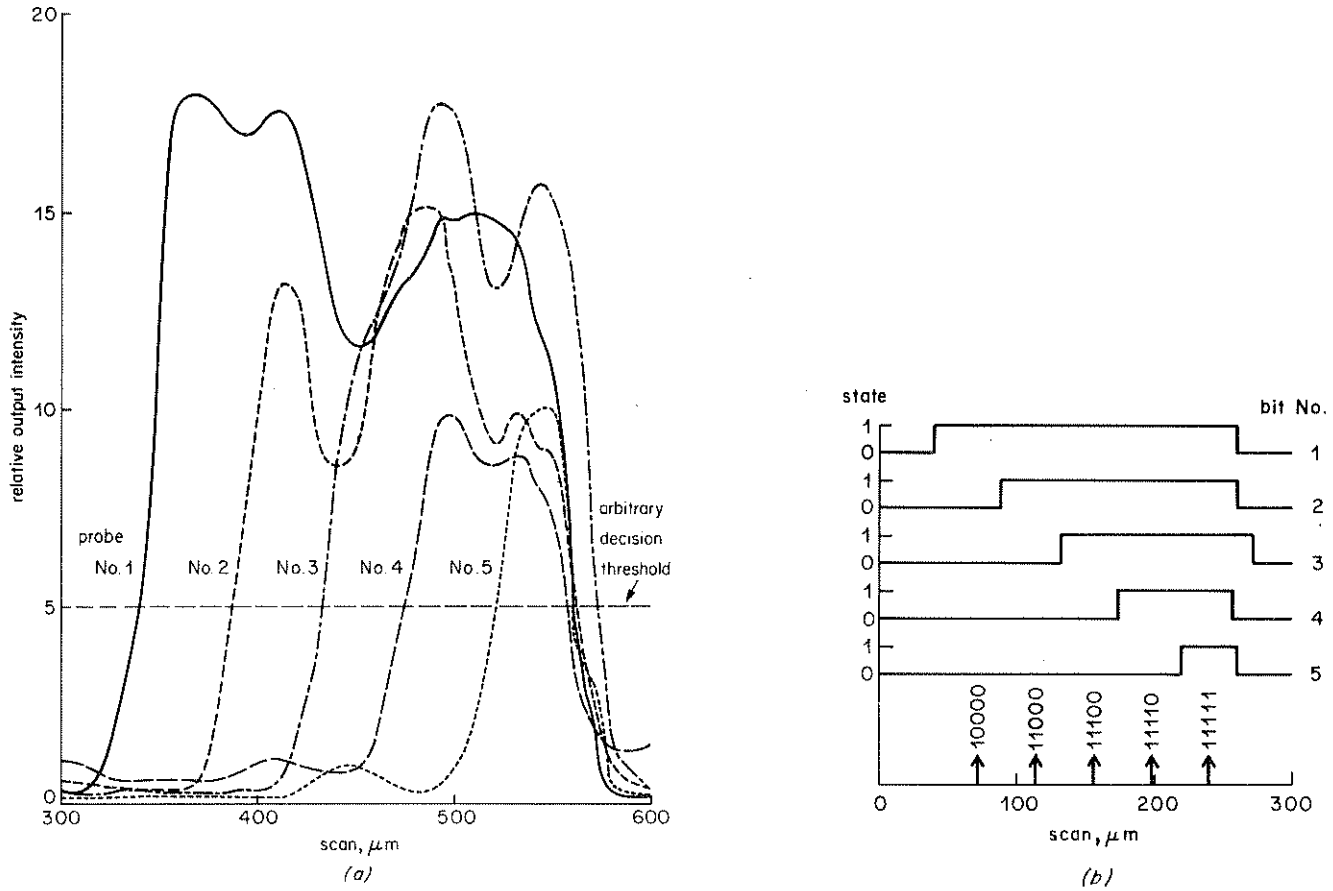

Fig. 17 - Reconstruction profiles for a row of 5-bit micro-holograms

(*a*) Measured relative intensities at each of the wanted image positions during a scan of five adjacent holograms

(*b*) Expected binary state profiles assuming an arbitrary on/off decision threshold in Fig. 17(*a*)

obtained by increasing the maximum spatial frequency to 160 cycles/mm, allowing a greater separation of the apertures.

Another difficulty encountered when regularly spaced apertures occur in lines is that the range of intensities in the exposure of the hologram can greatly exceed the useful range provided by the emulsion transfer characteristics. As the number, N, of screen apertures increases, spiky peaks of intensity proportional to N^2 occur, which are 'crushed' in the recording process and give rise to additional crosstalk in the reconstruction. The intensity range of the exposure can be substantially reduced by deliberately altering the relative phases of the light from each aperture prior to mutual interference in the hologram plane. This can be achieved by defocusing, i.e. by moving the film slightly away from the true Fourier-transform plane, or by altering the path lengths of the light passing through the apertures by means of a random phase plate. The latter appears to be the more satisfactory method for micro-hologram arrays.

Table 2 shows the reconstruction efficiency obtained with the Agfa 10E 75 emulsion for a 9-bit hologram, 30 μm in diameter, using a maximum spatial-frequency of 160 cycles/mm. As previously, the last column in Table 2 indicates the maximum theoretical efficiency.

4.3. Copying

A potential advantage of data recording using low spatial-frequency holograms is that copies could be taken using conventional printing techniques. Clearly, emulsions with high resolution characteristics need to be used for the prints. A brief experiment was carried out in which a row of 9-bit holograms, recorded on the Agfa 10E 75 emulsion, was contact printed on the same stock but with modified development characteristics; ordinary (tungsten) light was used for the exposure. A similar reconstructed image was obtained with the copied (positive) holograms, but there was a noticeable increase in crosstalk and a decrease in signal-to-background ratio, largely due to the extra blemishes caused by dust and scratches in the process.

More work is required to determine the most suitable copying technique; if an original recording of digital data can be produced with a sufficiently low error rate on read-out, perhaps the best approach would be simply to replay and re-record.

5. Conclusions

The analysis of spot-hologram formation and recording on film, supported by several basic experiments, indicates that information storage densities of 10^6 bits/cm^2 are feasible with average signal-to-interference ratios of 20 dB or better in the reconstruction, and with hologram spatial-frequency bandwidths of less than 200 cycles/mm. This value of storage density would allow a full-bandwidth colour television signal, coded in p.c.m. form (8 bits/sample), to be recorded with the same consumption of medium as that required for a conventional analogue recording on 35 mm cine-film. However, only a black-and-white film emulsion is required which, when suitably processed, is attractive for archival storage applications. Greater storage densities are theoretically possible by increasing the hologram bandwidth, and the holographic advantage of defect resistance is improved by increasing the spot area of each hologram spot in the array. The optimum number of bits per hologram spot, for digital television recording in real-time, will depend finally on the development of a suitable scanning method in conjunction with arrays of fast-acting light switches. This latter subject will form the next phase of this feasibility study.

The measured modulation transfer functions of several photographic emulsions used for high-resolution photography and line-recording proved to be rather inadequate for micro-holograms with bandwidths greater than about 100 cycles/mm. Far superior results were obtained using a commercially-available holographic film, but its sensitivity is about one order lower. Even so, for this slower holographic film, it is estimated that real-time recording at an information transfer rate of 100 Megabits/sec can be achieved with laser radiation powers less than 10 mW. This figure assumes a packing density of 10^6 bits/cm^2 or greater and an optical efficiency of the recording apparatus better than 10%. A similar order of laser power is required for the reconstruction process. Hence low-power Helium Neon gas lasers would be suitable light sources, and these are now available at relatively low cost and with a tube life in excess of 5000 hours.

The experimental work shows that the exposure latitude for recording micro-holograms is rather small (±½ stop) and this may present some operational difficulties bearing in mind possible batch-to-batch variations in film sensitivity. It was envisaged initially, that, by recording micro-hologram arrays with a conventional aspect ratio, a faint analogue version of the picture could be simultaneously overlayed on the digital recording; this additional intensity variation could occupy most, if not all, the exposure latitude and may not be practicable.

TABLE 2
9-bit, 30 μm diameter holograms

Emulsion type	M.T.F. at 150 cycles/mm	Hologram spacing μm	Diffraction Efficiency % (average per bit)	
			Measured	Theoretical (Max.)
Agfa 10E 75	0·85	30	0·34	0·6

6. References

1. RAJCHMAN, J.A. 1970. Holographic optical memory: an optical read-write mass memory. *Applied Optics*, 1970, **9**, 10, pp. 2269 – 2271.

2. MEZRICH, R.S. 1970. Magnetic holography. *Applied Optics*, 1970, **9**, 10, pp. 2275 – 2279.

3. LIN, L.H. *and* BEAUCHAMP, H.L. 1970. Write-read-erase in situ optical memory using thermoplastic holograms. *Applied Optics*, 1970, **9**, 9, pp. 2088 – 2092.

4. Possible techniques for the recording of digital television signals. BBC Research Department Report No. 1969/42.

5. BRIGGS, D.A., HACHFELD, K.D., REID, D.C.J. *and* WATERWORTH, P. 1970. A holographic data storage system. *Systems Technology*, 1970, No. 9, pp. 29 – 32.

6. LEITH, E. *and* UPATNICKS, J. 1964. Wavefront reconstruction with diffused illumination and three-dimensional objects. *J. Opt. Soc. Am.*, 1964, **54**, 11, p. 1295.

7. TAYLOR, E.W. BBC Research Department Report in course of preparation.

8. British Patent Application No. 7954/71.

9. BLACKMER, L.L., VANKERKHOVE, A.P., BALDWIN, R.E. *and* STULTZ, K.F. 1970. Some aspects of multiple-beam interference techniques in digital data recording. *Applied Optics*, 1970, **9**, 12, pp. 2753 – 2761.

10. BORN, M. *and* WOLF, E. 1959. Principles of optics. London, Pergamon, 1959.

11. BESTENRIENER, R., GREIS, U. *and* WEIER-SHAUSEN, W. 1971. Alphanumeric storage capacity of a defocused Fourier hologram matrix. *Phot. Science and Engineering*, 1972, **16**, 1, pp. 4 – 15.

SMW/JUC

Printed by BBC Research Department, Kingswood Warren, Tadworth, Surrey